

Metals under condition relevant to transient events in ITER

Yu V Martynenko

NRC «Kurchatov Institute», 1 Kurchatov sq., Moscow 123098, Russia
National Research Nuclear University MEPhI (Moscow Engineering Physics
Institute), 31 Kashirskoe highway, Moscow 115409, Russia

Corresponding author e-mail: martyn907@yandex.ru

Abstract. Droplet erosion and shielding plasma layer are shown to be closely connected and should be considered together self consisted. Droplet erosion is caused by plasma flow over the melt metal surface. Shielding plasma is produced from droplets evaporation. Experimental data analysis and theoretical models for these processes are presented.

1. Introduction

Problem of divertor and first wall erosion is a key problem for ITER creation. These tokamak components are loaded by the most intensive plasma heat action at transient phenomena such as plasma disruption and ELM. Heat load on ITER divertor at ELM is expected to be $Q = 0.2 - 5 \text{ MJ/m}^2$ at pulse duration $\tau = 0.1 - 1 \text{ ms}$, and at plasma disruption to be $Q = 10 - 100 \text{ MJ/m}^2$ at $\tau = 1 - 10 \text{ ms}$ [1, 2]. Plasma accelerator QSPU has plasma flow with parameters like those expected in ITER at disruption and ELMs [3]. However, pressure of QSPU plasma flow is several atmospheres, whereas pressure of plasma flow at ELM is expected to be $10^2 \div 10^3 \text{ Pa}$ and at disruptions to be $10^2 \div 4 \cdot 10^3 \text{ Pa}$. The most destructive damages for divertor is breaking, studied in [4], as well as the melt layer fast transport from one place to the other [5,6]. The latter phenomenon results in the most intensive thinning of plasma facing material. Droplet erosion at temperature below boiling temperature is the main mechanism of metal mass loss.

2. Metals erosion data analysis

The works [7,8] show that energy absorbed by target reaches saturation when power density of the initial plasma flow increases, provided absorbed energy density at saturation for tungsten and graphite equals approximately the same value $Q_{\text{abs}} = 0.4 \div 0.5 \text{ MJ/m}^2$. However at power density of the initial plasma flow corresponding to adsorbed energy saturation, mass losses of metals start to grow [9]. Evaporation from the surface, considered as the main mechanism of mass loss [10], is not high because movement of melt metal layer does not permit temperature to rise above the melting temperature (see Table I). Droplets seen during the pulses [9] allow us to propose that droplet erosion is the main reason of mass loss. However, emission of 100 droplets per pulse with average size $\sim 30 \mu\text{m}$ from target 6 cm diameter at $Q = 1.6 \text{ MJ/m}^2$ [9] corresponds to the specific mass loss $\Delta m \approx 2 \cdot 10^{-2} \text{ g/m}^2$, whereas measured mass loss at $Q = 1.6 \text{ MJ/m}^2$ was $\Delta m \approx 5 \text{ g/m}^2$ per pulse. In earlier work [12] on plasma accelerator MKT with short pulse $60 \mu\text{s}$, but high energy density 300 kJ/m^2 much more intensive droplets emission was observed (see figure 1). The droplets size emitted at MKT pulse was $\sim 1 \mu\text{m}$ and below. Estimate shows that mass loss caused by small droplets emission is much more than that caused by large droplets ($\sim 30 \mu\text{m}$) and can explain observed mass loss. In work [6] two



mechanisms of droplet emission were pointed. Both mechanisms are sequences of the plasma flow over melt metal surface, which leads to Kelvin-Helmholtz instability and waves on the surface.

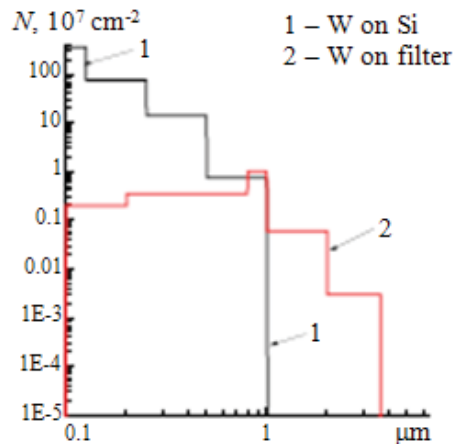


Figure 1. Size distribution of tungsten droplets at exposition in plasma accelerator MKT at $Q = 0.3 \text{ MJ/m}^2$ $\tau = 60 \text{ } \mu\text{s}$, 10 pulses. Droplets were collected: 1 - on Si collector capturing droplets flying parallel to the target surface, 2 - on basalt filter capturing droplets flying normal to target surface.

The first mechanism [13] is blowing out the wave crests by the plasma wind. In the work [13] this mechanism was believed to be responsible for small $\sim 1 \text{ } \mu\text{m}$ droplets emission. The second mechanism is a result of moving wave instability, which leads to one wave intercepting another one resulting in droplets emission. This mechanism explains emission of droplets with size 30—60 μm .

3. Waves on the melt metal surface and droplet emission

Waves emerged due to Kelvin—Helmholtz instability suggests existence of plasma flow over the melt metal surface [14]. In this case wave length λ , frequency ω and increment γ are the following

$$\lambda = 3\pi\alpha/2P \tag{1}$$

$$\omega = (2^{5/2}/3) \cdot (P^{3/2}/\alpha\rho^{1/2})(\rho'/\rho)^{1/2}, = 1.9 \cdot (P^{3/2}/\alpha\rho^{1/2})(\rho'/\rho)^{1/2} \tag{2}$$

$$\gamma = (2^{5/2}/3^{3/2}) P^{3/2}/\alpha\rho^{1/2} \approx 1.09 \cdot P^{3/2}/\alpha\rho^{1/2}, \tag{3}$$

where α is the surface tension, ρ' and U are the density and the velocity of plasma flow, respectively, ρ is the metal density, $P = \rho'U^2/2$ is the pressure of plasma flow. It is noticeable that $\omega \ll \gamma$ by $(3\rho/\rho')^{1/2} \approx 10^3$ times, in the most cases $\omega \sim 1/\tau$ and motion of waves is not possible. At pulse duration τ waves can arise only if $\gamma > 1/\tau$. This condition means that $P > P_{cr} = 0.94 \cdot \alpha^{2/3} \cdot \rho^{1/3} \cdot \tau^{2/3}$. At $\tau = 1 \text{ ms}$ the pressure of plasma flow should be $P > 7 \cdot 10^3 \text{ Pa}$ for tungsten, ($\lambda_{max} = 0.15 \text{ mm}$), and $P > 2.2 \cdot 10^3 \text{ Pa}$ for beryllium, ($\lambda_{max} = 3 \text{ mm}$).

Let us consider droplets emission as a result of the wave crests blowing out. The velocity of plasma flow over the waves is much higher than the velocity of wave motion. The plasma wind acts on the wave crest. Due to the viscosity the wave crest with height Δ can be considered as liquid on the solid substrate during the time t

$$t = \Delta^2/\nu \tag{4}$$

where ν is the kinematic viscosity. If this wave crest is shifted for the time t on the distance equal the length of wave crest base d , this wave crest will be taken away as droplets. If the plasma wind pressure is balanced by surface tension [6], the length of wave crest base d equals

$$d = (\Delta r)^{1/2}, r = \alpha d P \quad (5)$$

The time of wave crest shift on the distance d is

$$t = (2dl/a)^{1/2}, a = P \Delta / \rho \Delta d = P / \rho d \quad (6)$$

where a is the wave crest acceleration. The wave crest height can be found from (4), (5) and (6),

$$\Delta = (2\alpha\rho\nu^2)^{1/3} P^{2/3} \quad (7)$$

It is noticeable that velocity of the wave crest reaches the value $v = P \Delta^2 / \rho \nu d$, at which the plasma wind force equals to the friction force, just for the time of the crest shift. This means that the wave crest shift occurs in the regime of acceleration. Blowing away of one wave crest occurs after the previous wave crest is blown away in the time t . The wave height is limited by the crests removing and equals to $H = \Delta / \gamma$. The crest is removed from the whole front of the wave, and then the crest is divided into droplets with the volume $\sim (\Delta d)^{3/2}$ each. So blowing away of the crest from the wave with radius R results in appearance of $\pi R / (\Delta d)^{1/2}$ droplets with size

$$r = (\Delta d)^{1/2} = (2\rho)^{1/4} (\alpha\nu)^{1/2} P^{-3/4} \quad (8)$$

Droplets size decreases with the plasma wind pressure increase P . Droplets emitted in the region with maximal P have the smallest size. Droplets at the edge of plasma flow region where $P \approx P_{cr}$ have the maximal size. Table I shows that blowing away of the wave crests also results in large droplets emission. Number of droplets emitted from an area unit per pulse is

$$N_{dr}(P) = (\pi t) / (\lambda r) = \alpha 2^{1/12} / (3\pi) (\nu^{5/6} \alpha^{13/6} \rho^{11/12})^{-1} \cdot P^{37/12} \quad (9)$$

If the pressure distribution is $P \sim P_0 \cdot \exp(-R^2/\sigma^2)$, one can find the size distribution $N_{dr}(r)$ of droplets

$$N_{dr}(r) = dN_{dr}/dR \cdot 2\pi R \cdot dR/dr \approx \tau \nu^{23/18} \cdot \alpha^{1/9} \cdot \rho^{1/9} \cdot P_0^{37/24} \cdot \sigma^2 \cdot r^{-46/9} \quad (10)$$

Mass loss is determined by the small droplets emission and mass loss per pulse is

$$\Delta m = \rho \int r^3 \cdot (dN_{dr}/dr) \cdot dr \sim P_0^{25/8} \quad (11)$$

Mass loss grows steeply with the growth of the plasma flow pressure in accordance with [5]. The table I gives characteristics of droplets emission and mass loss for tungsten and beryllium at the initial plasma flow pressure corresponding to the energy density flow exceeding twice the threshold energy density for melting.

Table 1. The number of droplets emitted per QSPU pulse with $\tau = 0.5$ ms (N); the mass loss per pulse calculated with formula (11) (Δm), the mass loss caused by evaporation from the surface (Δm_{vapor}) and the mass loss measured experimentally [5] (Δm_{exp}), the maximal size of droplets emitted at wave crest blowing away (r_{max}).

	N, m^{-2}	$\Delta m, \text{g/m}^2$	$\Delta m_{\text{vapor}}, \text{g/m}^2$	$\Delta m_{\text{exp}}, \text{g/m}^2$	$r_{\text{max}}, \mu\text{m}$
W, $P_0 = 3$ atm	$5 \cdot 10^{12}$	20	$6 \cdot 10^{-2}$	$3 \div 9$	30
Be, $P_0 = 2$ atm	$4 \cdot 10^{14}$	10	$(4.5 \div 7) \cdot 10^{-3}$	$0.1 \div 0.35$ ($P \approx 1$ atm)	37

4. Near surface layer of shielding plasma

Instability development and waves on the melt metal surface are caused by the near surface plasma layer. The thickness of this layer is higher than the wave length, but the parameters of this layer differ

from the parameters of the shielding layer at ~ 1 cm from the metal surface [8]. Therefore we believe that the thickness of the near surface plasma layer is $L \sim 1$ mm.

The saturation of the energy absorbed by target means that the near surface plasma layer is optically thick. In this case temperature T of the near surface plasma layer can be calculated as $T = (W_{\text{abs}}/\sigma)^{1/4}$, where σ is the Stephan-Boltzmann coefficient, $W_{\text{abs}} = Q_{\text{abs}}/\tau$ is the absorbed power at saturation. At $W_{\text{abs}} \approx 1\text{GW/m}^2$ [8], $T \approx 1$ eV. The energy of the particle flow to the surface is much less than the radiation energy. We will believe that the temperature of the near surface plasma layer is constant $T \approx 1$ eV. The main mechanism of the target mass loss is droplet erosion, and we believe that droplets evaporation in the near surface plasma layer is the main source of the vapor for shielding plasma. The estimate shows that tungsten droplet flying from the surface evaporates if its size is $r < 1$ μm . The larger droplets decrease the size by $\sim \mu\text{m}$. At the constant temperature of the near surface layer the pressure in this layer is determined by the plasma density. The density of the near surface layer can be calculated from the condition of the flow continuity. At normal extension of the shielding plasma the density of the near surface plasma layer is $n = q/v_{\text{exp}}$, where $q = \Delta m/M\tau$ is the flow of vapor caused by droplets evaporation, M is the metal atom mass. Small droplets contribute the most to mass loss. Therefore we take Δm from the experimental mass loss. The velocity of plasma extension is $v_{\text{exp}} = [v_T^2 - P_{\text{ext}}/\rho']^{1/2}$, where v_T is the heat velocity, P_{ext} is the external pressure. Then the pressure in the near surface plasma layer is

$$P = P_{\text{ext}}/2 + [(P_{\text{ext}}^2/4) + (Mqv_T)^2]^{1/2} \quad (11)$$

The formula (11) shows that at $q > P_{\text{cr}}/2Mv_T$, even at $P_{\text{ext}}=0$, the pressure in the near surface layer is sufficient for tangential plasma flow, which can cause waves to appear and droplets to erode.

There are some examples when the instability of the melt metal layer and their sequences were observed at the pressure of initial plasma flow below critical: (i) droplets emission observed in [11] (figure 1) occurs at the pressure of initial plasma flow lower than required for development of the wave structure and droplet erosion. The pressure of MKT plasma flow was 10^3 Pa, whereas critical pressure for Kelvin-Helmholtz instability on tungsten is $P_{\text{cr}} = 7 \cdot 10^3$ Pa, (ii) other evidence of the shielding plasma influence on droplet emission is time dependence of droplets ejection obtained in [5]. The main droplets emission occurs after QSPA pulse completion. Pulse duration was 0.5 ms, whereas maximal droplet emission was observed at 1 ms and droplet emission lasted up to 2 ms. This means that droplet emission was initiated by the shielding plasma which regenerates itself by droplets evaporation, (iii) the best evidence of the shielding plasma action is simulation of the disruption mitigation on QSPA [4]. In this case, QSPA plasma flow acts on Ar gas target and Ar radiation acts on stainless steel. Radiation has zero pressure but the observed wave structure is a result of shielding plasma flow over the melt metal surface.

However, development of the Kelvin-Helmholtz instability without external pressure is possible not in all cases. Calculation and experiment [11] show that erosion of beryllium is low and $q < P_{\text{cr}}/2Mv_T$. Experiments on plasma accelerator QSPU-Be in Bochvar Research Institute of Inorganic Materials [11] show that the wave relief and the melt metal movement on Beryllium is observed only after direct plasma action on the Be target. After radiation pulses with the same energy the wave structure was absent. Instability development at the absent external pressure is possible at the normal initial plasma flow and normal shielding plasma extension. At the sliding initial plasma flow and at magnetic field the shielding plasma expansion occurs otherwise. These cases are to be considered specially.

Acknowledgements

This work was supported in part by National Research Nuclear University MEPhI in the framework of the Russian Academic Excellence Project (contract No. 02.a03.21.0005, 27.08.2013).

References

- [1] ITER Physics Basis 1999 *Nucl. Fusion* **39** 2137

- [2] Federici G, Skinner C H, Brooks JN et al. 2001 *Nucl. Fusion* **41** 1967
- [3] Würz H, Arkhipov N I, Bakhtin V P, Safronov V M et al. 1995 *J. Nucl. Mat.* **220—222** 1066
- [4] Budaev V P, Martynenko Yu V, Khimchenko L N, Zhitlukhin A M, Klimov N S, Pitts R A, Linke I, Belova N E, Karpov A V, Kovalenko D V, Podkovyrov V L and Yaroshevskay A D 2013 *Plasma Phys. Reports* **39** 910
- [5] Poznyak I M, Klimov N S, Podkovyrov V L, Safronov V M, Zhytlukhin A M and Kovalenko D V 2012 *PAST Ser. Thermonuclear Fusion* **4** 23
- [6] Martynenko Yu V 2014 *PAST Ser. Thermonuclear Fusion* **37** (2) 53
- [7] Safronov V M, Arkhipov N I, Landman I S, Pestchanyi S E, Toporkov D A and Zhitlukhin A M 2009 *J. Nucl. Mat.* **386—388** 744
- [8] Poznyak I M, Arkhipov N I, Karelov S V, Safronov V M and Toporkov D A 2015 *International Summer School on the Physics of Plasma-Surface Interaction* Moscow, MEPhI
- [9] Klimov N S, Podkovyrov V L, Zhitlukhin A M, Safronov V M, Kovalenko D V, Moskacheva A A and Posnyak I M 2009 *PAST Ser. Thermonuclear Fusion* **2** 52
- [10] Krasheninnikov S I, Pigarov A Yu and Lee Wonjae 2015 *Plasma Phys. Control. Fusion* **57** 044009
- [11] Safronov V M *Private communication*
- [12] Guseva M I, Gureev V M, Domantovskii A G, Martynenko Yu V, Moskovkin P G, Stolyarova V G, Strunnikov V M, Plyashkevich V and Vasilev V I 2002 *J. Techn. Phys.* **72** 7841
- [13] Martynenko Yu V and Moskovkin P G 2000 *PAST Ser. Thermonuclear Fusion* **1** 65
- [14] Landau L D and Lifshits E M 1988 *Hydrodynamics* **6** (Moscow: Nauka)